Available online at www.sciencedirect.com
ScienceDirect
Journal of Power Sources 170 (2007) 55–60
JOURNAL OF POWER SOURCES
www.elsevier.com/locate/jpowsour

Short communication

NiO/YSZ, anode-supported, thin-electrolyte, solid oxide fuel cells fabricated by gel casting

Lan Zhang [a,b], San Ping Jiang [b,*], Wei Wang [b], Yujun Zhang [a]

[a] *Key Laboratory for Liquid Structure and Heredity of Ministry of Education, School of Material Science and Engineering, Shandong University, Jinan 250061, China*

[b] *School of Mechanical and Aerospace Engineering, Nanyang Technological University, Singapore 639798, Singapore*

Received 6 January 2007; accepted 19 March 2007
Available online 20 April 2007

Abstract

A simple and cost-effective gel-casting technique is developed and optimized to fabricate NiO/stabilized yttria–zirconia (YSZ) anode-supported solid oxide fuel cells (SOFCs). The effect of ammonium poly-(methacrylate) (PMAA) dispersant and pH on the zeta potential of YSZ and NiO particles and the viscosity of the NiO/YSZ slurries is studied in detail. The results show that the absolute zeta potential of YSZ and NiO particles reaches a maximum value at pH value ∼10 and the viscosity of the NiO/YSZ slurry is lowest when the PMAA dispersant content is 1.5 wt.%. A gel-cast NiO/YSZ anode-supported button cell with a spin-coated, thin, YSZ electrolyte film (∼9 μm) and a $La_{0.72}Sr_{0.18}MnO_{3-\delta}$ (LSM)/YSZ composite cathode gives a peak power output of 1.07 and 0.65 W cm^{-2} at 900 and 800 °C under humidified hydrogen and air. The effect of a graphite pore-former in the gelation and microstructure of NiO/YSZ anode substrates is investigated.

Keywords: Solid oxide fuel cells; NiO/stabilized yttria–zirconia (YSZ) anode substrates; Gel casting; Optimization; Peak power; Graphite pore-former

1. Introduction

Solid oxide fuel cells (SOFCs) have attracted considerable attention as efficient power-generating systems with very low greenhouse gas emissions and high fuel flexibility as compared with other fuel cell systems [1–3]. Currently, the commonly used materials are fully stabilized yttria–zirconia (YSZ) as the electrolyte, Ni/YSZ as the anode, doped $LaMnO_3$ as the cathode, and high temperature oxidation resistance alloys as the interconnect. Major technical problems facing SOFC developers include durability and thermal cycleability, corrosion of the metallic interconnect, and performance degradation. Most of these problems can be substantially reduced by lowering the operating temperature of the SOFC from 950–1000 °C to 600–800 °C.

One of the main challenges in lowering the operating temperature is the increase in the cell resistance and, consequently, losses in cell efficiency due to the rapid increase in the bulk resistivity of the electrolyte and in the electrode polarization resistance at the electrode|electrolyte interfaces [4–7]. As the resistivity loss of the electrolyte is one of the dominant factors affecting the performance of SOFCs, extensive efforts have been made to develop an anode-supported cell structure and to reduce substantially the thickness of the electrolyte to several tens of microns [6,8–15]. There are various techniques to fabricate anode substrates that include tape-casting [16,17], die-pressing [6,9–15] and coat-mixing processes [18]. Gel casting is a novel method in fabricating complex three-dimensional ceramic parts and offers a significant advantage in terms of better homogeneity and thus higher flexural strength in comparison with the conventional forming methods [19–21]. In this process, a slurry with a high solid loading is obtained by dispersing the ceramic powders in a pre-mixed monomer and cross-linking solution. With heating or addition of a catalyst, cross-linking polymerization occurs to form a three-dimensional network structure, and the slurry is solidified in situ, to form ceramic objects of the desired shape. Recently, gel casting has gained attention as a new method in the preparation of electrode powders [22–24] and electrode-supported substrates for SOFCs [25].

This paper presents the development of NiO/YSZ anode-supported SOFCs prepared by the gel-casting method. The effect

* Corresponding author. Tel.: +65 6790 5010; fax: +65 6791 1859.
E-mail address: mspjiang@ntu.edu.sg (S.P. Jiang).

0378-7753/$ – see front matter © 2007 Elsevier B.V. All rights reserved.
doi:10.1016/j.jpowsour.2007.03.080

of ammonium poly-(methacrylate) (PMAA) dispersant on the zeta potential of YSZ and NiO particles and the viscosity of NiO/YSZ slurry is examined. The results show that gel casting is an effective method to prepare high-performance NiO/YSZ, anode-supported, thin, YSZ electrolyte cells.

2. Experimental

2.1. Preparation of NiO and YSZ powder suspension and slurry

NiO (J.T. Baker, USA) and 8 mol% Y_2O_3–zirconia (YSZ, TOSOH, Japan) were used in this study. Before preparation of NiO/YSZ anode substrates by gel casting, the effect of dispersant and pH on the zeta potential of the NiO and YSZ particles and viscosity of NiO/YSZ slurry were investigated. A NiO suspension was prepared by mixing 0.34 g NiO in distilled water with and without the addition of ammonium poly-methacrylate dispersant (PMAA, SD-03, Jiangsu Huagui Hi-Tech Ceramics Co., China). The concentration of PMAA was 0.6 wt.% based on the solid content of NiO. A YSZ suspension was prepared in a similar manner. The total solid content in the suspension was 0.05 vol.%. The pH of the suspension was optimized by adding dilute HCl or NaOH solution. The zeta potential of NiO and YSZ particles was measured by a zeta potential analyzer (Brookhaven Instruments Corporation).

NiO powder calcined at 700 °C in air for 2 h was mixed with YSZ powder (NiO:YSZ = 65:35 by weight) in distilled water and ball-milled for 24 h. Graphite was added as a pore-former and the content was in the range of 5–15 wt.%. In the case of graphite pore-former, polyvinyl pyrrolidone (PVP, Sigma–Aldrich) was added to the slurry to promote the gelation process. The pre-mixed monomer solution was prepared from mono-functional acrylamide (AM, Sigma–Aldrich) and di-functional *N*,*N*′-Methylenebis-acrylamide (MBAM, Sigma–Aldrich); PMAA was added as dispersant. The NiO/YSZ/graphite mixture was then added to the pre-mixed monomer solution, followed by a planetary ball-milling for 30 min. The pH of the slurry was adjusted during the ball-milling process. The viscosity of NiO/YSZ slurry was measured by a rotary viscometer (NDJ-1 Shanghai, China).

2.2. Anode substrate and cell fabrication

Ammonium persulfate (APS, Sigma–Aldrich) and *N*,*N*,*N*′*N*′-tetra methyl-ethylene diamide (TEMED, Sigma–Aldrich) were added to the NiO/YSZ slurry as an initiator and a catalyst, respectively. The slurry was poured into a mould, and subsequently heated in an oven at 80 °C for 1 h. The gel was cut into discs, followed by drying at 60 °C for 24 h and at 80 °C for another 24 h. The as-prepared green anode-substrates were stored ready for use. A flow chart of the gel-casting process is given in Fig. 1.

The YSZ electrolyte thin film was prepared by a spin-coating method. A suspension of 10 wt.% YSZ in *iso*-propanol was spin coated on to the anode substrate at 1200 rpm for 15 s. The coating was dried at room temperature and the spin-coating process was repeated for several times. The YSZ-coated NiO/YSZ substrates were co-sintered at 1350 °C for 4 h to form a bilayer structure with a porous anode substrate and a dense electrolyte thin film. The anode substrate was ∼19 mm in diameter and ∼1.2 mm in thickness.

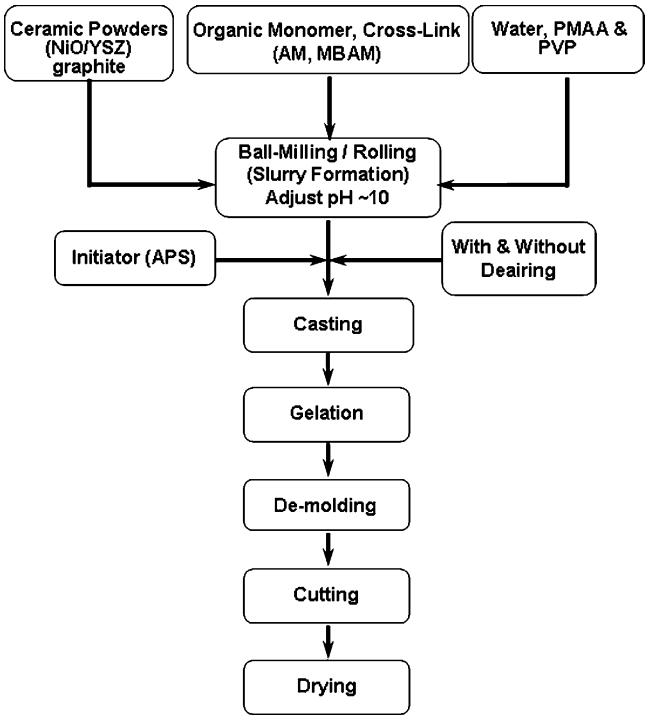

Fig. 1. Flow chart of gel-casting process for NiO/YSZ anode-substrates.

$La_{0.72}Sr_{0.18}MnO_{3-\delta}$ (LSM) cathode was synthesized by a water-based gel-casting process [26]. A LSM/YSZ composite cathode (LSM:YSZ = 60:40, w:w) was applied to the NiO/YSZ/YSZ bi-layer substrate by means of a slurry painting method. A pure LSM layer was applied to the surface of the LSM/YSZ composite to serve as a current-collector. The cathode area was 0.5 cm^2. The LSM/YSZ compositesive cathode was sintered in air at 1150 °C for 2 h.

2.3. Cell testing

The cell performance was evaluated with a built-in-house test station. The cell was sealed between two alumina tubes with a ceramic paste. During the test, hydrogen humidified at room temperature (3% H_2O/97% H_2) was fed to the anode chamber at a flow rate of 100 sccm, while the cathode was exposed to an air flow rate of 100 sccm. Electrochemical measurements were performed by means of a Solartron 1260 frequency response analyzer in conjunction with a 1287 electrochemical interface. The overall cell impedance was measured in the frequency range of 100 kHz to 0.01 Hz with a signal amplitude of 10 mV at open-circuit over a temperature range of 600–900 °C. Newly prepared cells were activated under a constant current of 200 mA cm^{-2} at 800 °C for 4 h before measurement [9]. The microstructure of the cell after the test was examined by scanning electron microscopy (SEM, Leica 360).

3. Results and discussion

3.1. Effect of pH value on zeta potential of YSZ and NiO particles

The effect of pH on the zeta potential of the YSZ and NiO particles in water and in 0.6 wt.% PMAA dispersant is shown in Fig. 2. The absolute zeta potential for the YSZ particles increases with increase in pH and reaches a maximum when the pH is ~10. The maximum value of the absolute zeta potential is 51 mV and 100 mV in water without and with the addition of PMAA dispersant, respectively (Fig. 2a). The NiO particles also reach a maximum absolute zeta potential at a similar pH value (Fig. 2b). In both cases, the absolute zeta potential in the PMAA dispersant solution is significantly higher than that in pure water. According to the electrostatic stabilization theory [27], a high absolute value of zeta potential in the suspension indicates an increase in the electrostatic forces between the particles, which will lead to high stability of the YSZ and NiO suspensions. In another words, the most stable NiO/YSZ slurry is obtained when the pH value is adjusted to ~10.

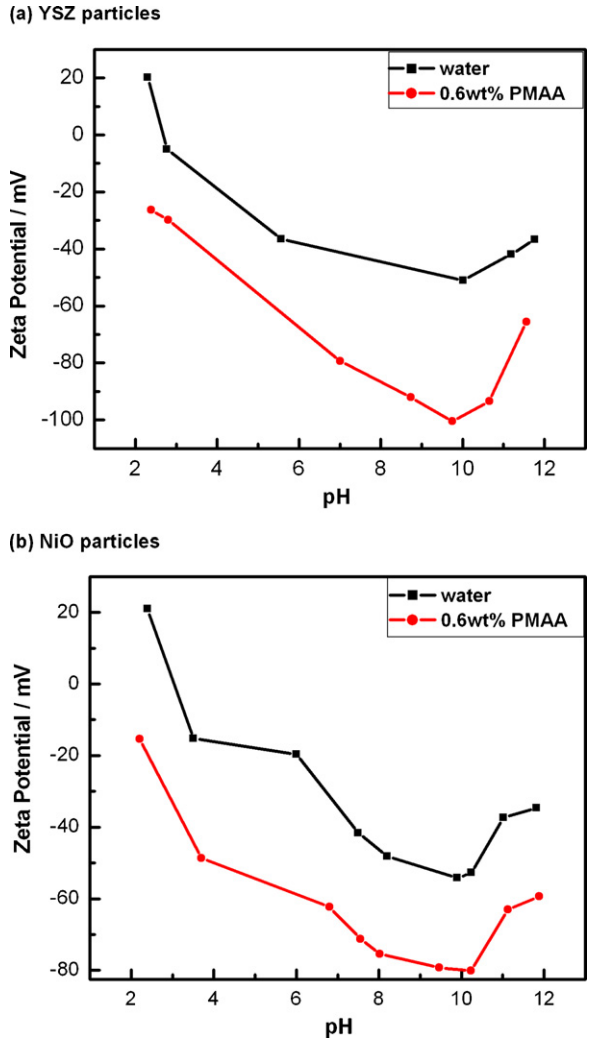

Fig. 2. Zeta potential of (a) YSZ and (b) NiO particles in water and in 0.6 wt.% PMAA dispersant solution at different pH values.

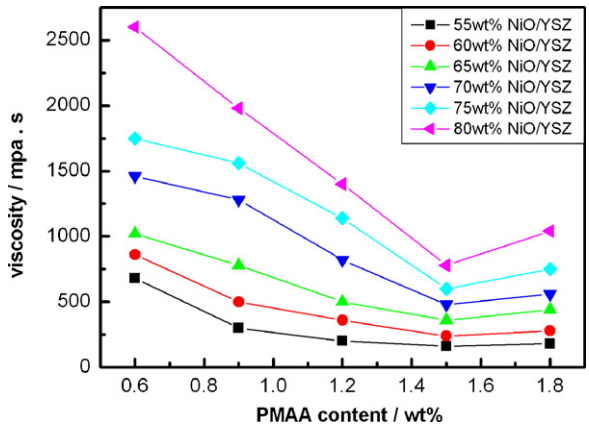

Fig. 3. Effect of PMAA dispersant content on viscosity of NiO/YSZ slurry as function of NiO/YSZ solid loading.

3.2. Effect of dispersant content on viscosity of NiO/YSZ slurry

An important parameter for the gel-casting process is a stable slurry with a high solid loading [28,29]. A low solid loading and an unstable slurry will result in high shrinkage and precipitation with the formation of surface cracks and bulk defects in the ceramics. In order to obtain a NiO/YSZ slurry with a high solid loading and low viscosity, PMAA dispersant was added. The effect of PMAA content on the viscosity of NiO/YSZ slurry as a function of the NiO/YSZ solid loading is presented in Fig. 3. The viscosity increases with the NiO/YSZ solid content. By contrast, the viscosity of slurry decreases significantly with increasing PMAA dispersant content and reaches a minimum at ~1.5 wt.% for a NiO/YSZ solid loading as high as 80 wt.%. The viscosity increases again when the dispersant content is higher than 1.5 wt.%.

Addition of PMAA dispersant reduces the agglomeration and improves the dispersion of NiO and YSZ particles. This is supported by a significant decrease in the viscosity of the NiO/YSZ slurry with increase in PMAA dispersant (Fig. 3). On the other hand, PMAA is a polymer with long ophidian chains and thus chain entanglement could also increase the viscosity. This appears to explain the V-shape dependence of viscosity of the NiO/YSZ slurry on PMAA content [30].

3.3. Effect of graphite content on stability and gelation of slurry

In anode-supported solid oxide fuel cells, the anode substrate must have sufficient porosity to allow gas diffusion and transportation to the reaction sites. As the gel-casting method is traditionally employed to produce dense ceramic objects [19–21], it is necessary to add the graphite pore-former to increase the porosity of the substrates.

Zhu et al. [31] showed that the absolute zeta potential for graphite also reaches the maximum value of 35 mV at the pH value of 9–10, which is similar to that observed for the NiO and YSZ particles in the present study. It has been found, however, that graphite has a detrimental effect on the polymerization reac-

tion of AM and MBAM. Thus, PVP was added to the NiO/YSZ slurry to promote the gelation process. The stability and the gelation of the slurry are significantly affected by the concentration of PVP. When the PVP concentration is low, graphite powder is separated from the slurry and accumulates on the surface of the slurry. This inhibits the gelation process. As the PVP concentration is increased, separation of graphite decreases and gelation of the slurry occurs easily. By contrast, the viscosity of the slurry increases with increase in PVP content. It is found that a trade-off between easy gelation and relatively low viscosity is obtained at 5 wt.% PVP based on the graphite loading under the conditions of the present study.

Separation and accumulation of graphite from the NiO/YSZ slurry is most likely due to the hydrophobic and non-wetting nature of graphite. Adding PVP will increase the hydrophilicity of the graphite particles and thereby reduce the separation. When the PVP concentration is low, however, not all the graphite particles are coated by hydrophilic PVP molecules. Increasing the PVP content will increase the coverage of the graphite particles by PVP. At a critical PVP concentration (5 wt.% in this study), all the graphite particles will be covered by PVP and thus prevent graphite separation and promote the gelation process. Nevertheless, with further increasing PVP content, the extra PVP molecules in the slurry will increase the viscosity of the slurry, similar to that of PMAA.

3.4. Cell performance and microstructure

The open-circuit voltage (OCV) of the cell under conditions of 3% H_2O/97% H_2 fuel and air is ~1.092 V at 800 °C, which is close to the theoretical value of 1.105 V at 800 °C. This indicates that the electrolyte thin film prepared by spin coating is dense with no cross pores and cracks. The cell performance measured at different temperatures under humidified H_2 and air is shown in Fig. 4. The cell was made from gel casting a NiO/YSZ substrate with the addition of 5 wt.% graphite pore-former. The maximum power density is 0.27, 0.45, 0.65, 0.84 and 1.07 W cm^{-2} at 700, 750, 800, 850 and 900 °C, respectively. These values are comparable with that of cells prepared by other

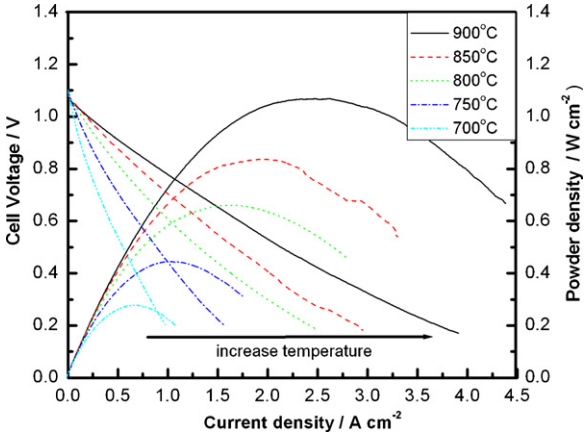

Fig. 4. Cell performance of gel-cast NiO/YSZ anode-supported thin-film YSZ cell at different temperatures (H_2: 100 sccm; air: 100 sccm).

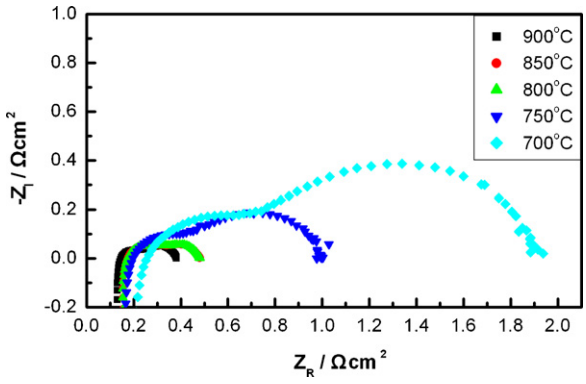

Fig. 5. Impedance spectra of gel-cast NiO/YSZ anode-supported thin-film YSZ cell measured at different temperatures under open-circuit (H_2: 100 sccm; air: 100 sccm).

techniques such as tape-casting. For example, Wang et al. [32] reported power outputs of 0.42 and 0.85 Wcm^{-2} for a tape-cast Ni–YSZ/YSZ/LSM–YSZ cell at 700 and 800 °C, respectively. The YSZ electrolyte was prepared by spray coating and the thickness was ~3 μm. In our cell, the YSZ electrolyte thickness is ~9 μm, i.e., triple the YSZ electrolyte thickness reported by Wang et al. [32]. By contrast, the power densities of the gel-cast anode-supported cell are lower than that of a cell prepared by the dry-pressing method [9]. This suggests that the cell performance can be improved further by optimization of the anode microstructure and electrode|electrolyte interface contact.

The impedance spectra of the gel-cast NiO/YSZ, anode-supported, thin YSZ electrolyte cell measured at different temperatures under open-circuit conditions are presented in Fig. 5. The impedance responses of the cell are characterized by a larger arc in the low-frequency range and a much smaller one in the high-frequency range. The overall electrolyte resistance of the cell (or the area specific resistance, ASR) was obtained from the high-frequency intercept while the total interfacial polarization resistance (R_P) of the cell was obtained from the difference between the high- and low-frequency intercepts. The apparent ASR of the cell is 0.25, 0.20, 0.18, 0.17 and 0.14 Ω cm^2 and the R_P is 1.69, 0.80, 0.44, 0.31 and 0.24 Ω cm^2 at 700, 750, 800, 850 and 900 °C, respectively.

The temperature dependence of the apparent ASR and R_P of the gel-cast, anode-supported, thin YSZ electrolyte cell is presented in Fig. 6. The corresponding values reported for a thin-YSZ electrolyte film deposited on NiO/YSZ anode substrates by spin coating [9,33], filter-coating [11], and spray coating [34] with a Ni/YSZ anode-support and a LSM/YSZ composite cathode are also included in Fig. 6. The activation energy values for ASR and R_P of the thin-electrolyte YSZ cells are listed in Table 1. The activation energy of the ASR of the YSZ thin film made by the spin-coating is 34 kJ mol^{-1}, which is significantly lower than the 87.5 kJ mol^{-1} reported for a bulk YSZ pellet [35]. Similar low activation energies have been observed by other workers (see Table 1). The significantly low activation energy of the cell ASR compared with that of the bulk YSZ pellet is most likely related to the fact that this parameter is strongly influenced by the electrode|electrolyte interfacial contact as well as the contact between the electrode and current-collector [36,37]. This

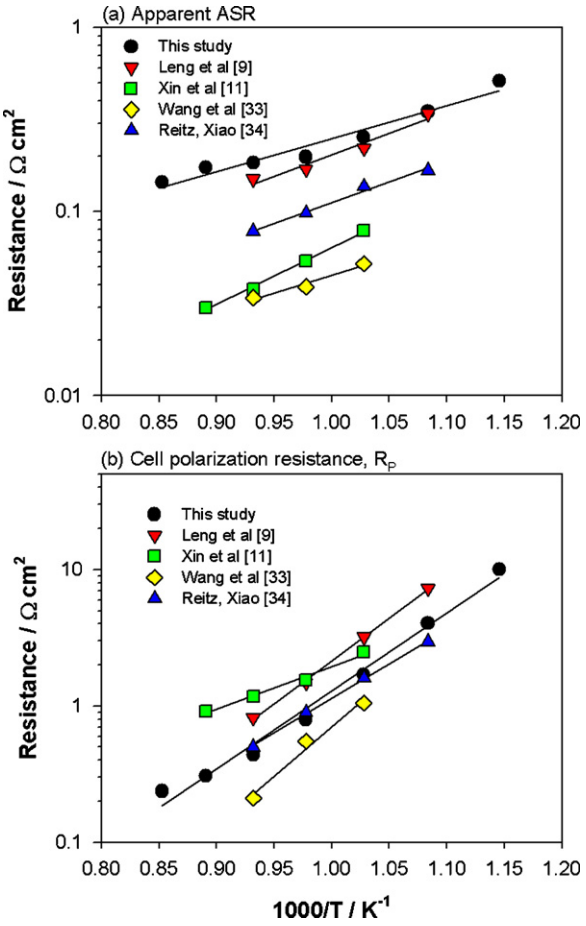

Fig. 6. Activation energy plots of apparent area specific resistance (ASR) and total polarization (interfacial) resistance of anode-supported thin-electrolyte YSZ cells. Resistance values measured from impedance spectra of cell under open-circuit conditions. Numbers are references cited.

is supported by the observation that the measured cell ASR is significantly higher than that calculated based on the YSZ electrolyte thickness. At 800 °C, the resistivity of YSZ is 18.18 Ω cm [38]. As shown below, the YSZ electrolyte thickness of the cell in this study is ~9 μm. This gives 0.0164 Ω cm^2 for the ASR of the YSZ electrolyte, which is substantially lower than 0.18 Ω cm^2, the apparent ASR measured at 800 °C. The activation energy values for the total polarization (interfacial) resistance are within the range of 97–139 kJ mol^{-1}. Apart form the low value reported by Xin et al. [11], these energies are generally lower than those of ~100–170 kJ mol^{-1} for H_2 oxidation on Ni/YSZ cermet anodes [39,40] and 160–270 kJ mol^{-1} for O_2 reduction on LSM and LSM/YSZ composite cathodes [41,42]. The reason for this difference not completely understood at this stage and requires further study.

Table 1
Activation energy of apparent area specific resistance (ASR) and total polarization (interfacial) resistance (R_P) of anode-supported thin-electrolyte YSZ cells

Activation energy (kJ mol^{-1})		Reference
Apparent ASR	R_P	
34	110	This work
45	121	[9]
59	60	[11]
37	139	[33]
43	97	[34]

Resistance values are measured from impedance spectra under open-circuit conditions.

Scanning electron micrographs of cross-sections of a gel-cast NiO/YSZ cell with a thin YSZ film and a LSM/YSZ composite cathode after testing are given in Fig. 7. The YSZ electrolyte film is dense with limited and isolated closed pores. The thick-

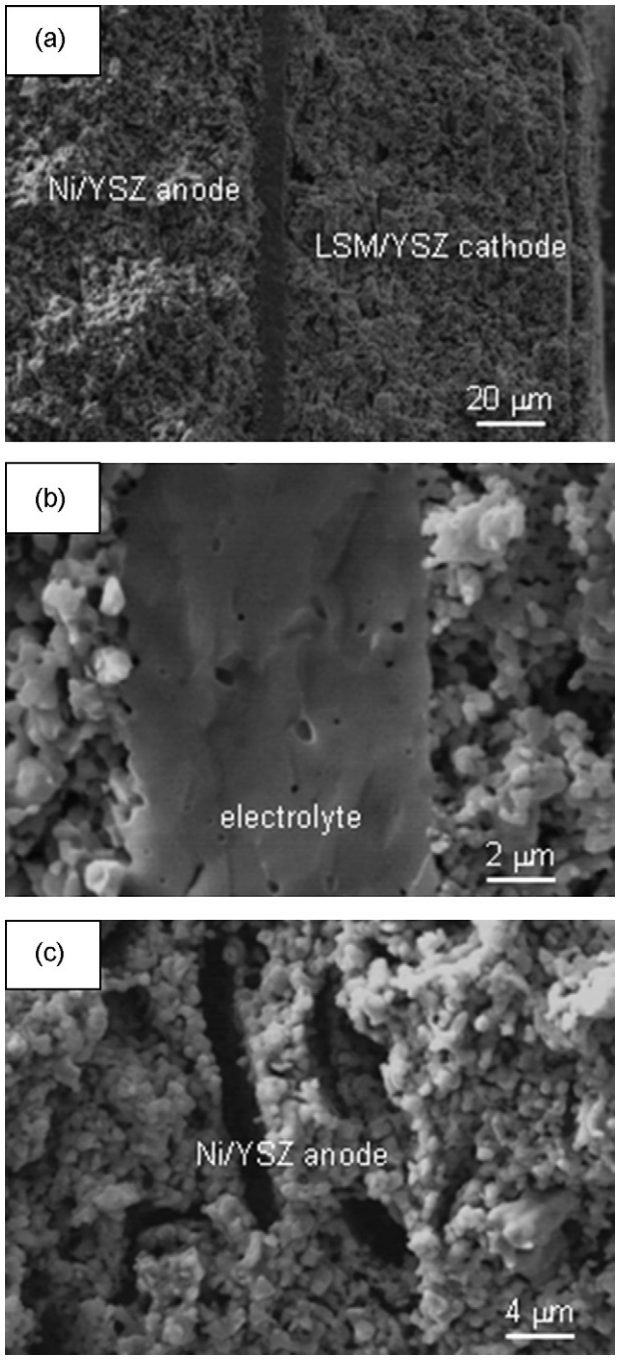

Fig. 7. Scanning electron micrographs of cross-section of a gel-cast Ni/YSZ anode-supported thin-electrolyte YSZ cell: (a) overview of cell; (b) electrolyte; (c) Ni/YSZ anode substrate.

ness of the YSZ electrolyte is ∼9 μm and the YSZ electrolyte adhers well to the gel-cast NiO/YSZ anode substrates (Fig. 7(b)). The thickness of the cathode is around 80 μm. For the gel-cast Ni/YSZ anode substrates, Ni and YSZ appear to be uniformly distributed. There are some large flake-shaped pores, which are probably due to the flake-shaped graphite pore-former. As shown by Boaro et al. [43], the pore structure and porosity of the YSZ are significantly affected by the shape and size of the pyrolyzable pore-formers. This clearly shows that the microstructure of the gel-cast Ni/YSZ substrates for the thin-electrolyte YSZ cell can be further improved and optimized. Nevertheless, the results in the present study demonstrate that the gel-casting method can be effectively used to fabricate high-performance, anode-supported, thin-electrolyte YSZ cells.

4. Conclusions

In this study, a gel-casting process has been optimized for the fabrication of NiO/YSZ anode substrates for intermediate-temperature SOFCs. The effects of PMAA dispersant and pH on the zeta potential of YSZ and NiO particles and the viscosity of the NiO/YSZ slurries has been studied in detail. The results show that the absolute zeta potentials of YSZ and NiO particles in water and dispersant solution reach maximum values at pH ∼10 and the viscosity of the NiO/YSZ slurry reaches a minimum when the content of PMAA dispersant is 5 wt.% in a NiO/YSZ solid loading range of 55–80 wt.%. Also, in the case of graphite pore-former addition, PVP is found to be effective in the prevention of graphite separation and the promotion of the gelation step. A gel-cast Ni/YSZ anode-supported button cell with a spin-coated thin YSZ electrolyte film (∼9 μm) and a LSM/YSZ composite cathode delivers a peak power output of 1.07 and 0.65 W cm^{-2} at 900 and 800 °C, respectively, under humidified H_2 and air. The cell performance can be further improved by optimizing the microstructure of the gel-cast anode substrates via proper selection of the pore formers and by improving the electrode|electrolyte interfacial contact to reduce the apparent ASR of the cell.

References

[1] T.L. Wen, D. Wang, M. Chen, H. Tu, Z. Zhang, H. Nie, W. Huang, Solid State Ionics 148 (2002) 513.
[2] N.Q. Minh, J. Am. Ceram. Soc. 76 (1993) 563.
[3] S.C. Singhal, K. Kendall, High Temperature Solid Oxide Fuel Cells: Fundamental, Design and Applications, Elsevier, Oxford, UK, 2003.
[4] X. Xu, C. Xia, S. Huang, D. Peng, Ceram. Int. 31 (2005) 1061.
[5] S. de Souza, S.J. Visco, L.C. de Jonghe, Solid State Ionics 98 (1997) 57.
[6] Y.J. Leng, S.H. Chan, S.P. Jiang, K.A. Khor, Solid State Ionics 170 (2004) 9.
[7] J. Will, A. Mitterdorfer, C. Kleinlogel, D. Perednis, L.J. Gauckler, Solid State Ionics 131 (2000) 79.
[8] J.W. Kim, A.V. Virkar, K.Z. Fung, K. Mehta, S.C. Singhal, J. Electrochem. Soc. 146 (1999) 69.
[9] Y.J. Leng, S.H. Chan, K.A. Khor, S.P. Jiang, Int. J. Hydrogen Energy 29 (2004) 1025.
[10] Q.L. Liu, K.A. Khor, S.H. Chan, J. Power Sources 161 (2006) 123.
[11] X.S. Xin, Z. Lü, X.Q. Huang, X.Q. Sha, Y.H. Zhang, W.H. Su, J. Power Sources 159 (2006) 1158.
[12] X.Y. Xu, C.G. Xia, S.G. Huang, D.K. Peng, Ceram. Int. 31 (2006) 1061.
[13] Y.Y. Chen, W.C.J. Wei, Solid State Ionics 177 (2006) 351.
[14] X.S. Xin, Z. Lü, X.Q. Huang, X.Q. Sha, Y.H. Zhang, K.F. Chen, N. Ai, R.B. Zhu, W.H. Su, J. Power Sources 160 (2006) 1221.
[15] L. Jia, Z. Lü, X.Q. Huang, Z.G. Liu, K.F. Chen, X.Q. Sha, G.Q. Li, W.H. Su, J. Alloys Compd. 424 (2006) 299.
[16] R. Cracium, S. Park, R.J. Gorte, J.M. Vohs, C. Wang, W.L. Worrell, J. Electrochem. Soc. 146 (1999) 4019.
[17] P.K. Srivastava, T. Quach, Y.Y. Duan, R. Donelson, S.P. Jiang, F.T. Ciacchi, S.P.S. Badwal, Solid State Ionics 99 (1997) 311.
[18] D. Simwonis, H. Thülen, F.J. Dias, A. Naoumidis, D. Stöver, J. Mater. Proc. Technol. 92/93 (1999) 107.
[19] T. Xunyan, Study on dispersion mechanisms and forming process of ZrO_2-based ceramic composite powder, Ph.D. Thesis, Shandong University, China, 2005.
[20] O.O. Omatete, M.A. Janney, R.A. Strehlow, Am. Ceram. Soc. Bull. 70 (1991) 1641.
[21] A.C. Young, O.O. Omatete, M.A. Janney, P.A. Menchhofer, J. Am. Ceram. Soc. 74 (1991) 612.
[22] Y.H. Yin, S.Y. Li, C.R. Xia, G.Y. Meng, Electrochim. Acta 51 (2005) 2594.
[23] X. Liu, G. Li, J. Tong, D. Chen, Ceram. Int. 30 (2004) 2057.
[24] J.-G. Cheng, S.-W. Zha, J. Huang, X.-Q. Liu, G.-Y. Meng, Mater. Chem. Phys. 78 (2003) 791.
[25] W.L. Huang, Q.S. Zhu, Z.H. Xie, J. Power Sources 162 (2006) 464.
[26] L. Zhang, Y. Zhang, Y.D. Zhen, S.P. Jiang, J. Am. Ceram. Soc., in press.
[27] J. Ren, J. Shen, S.C. Lu, Science and Technology of Particles Dispersion, Chemical Industry Press, Beijing, 2005, pp. 74–78.
[28] D. Guo, K. Cai, C. Nan, L.-T. Li, et al., Scripta Mater. 47 (2002) 383.
[29] D. Guo, K. Cai, L.-T. Li, et al., Ceram. Int. 29 (2003) 403.
[30] J. Tong, D. Chen, Ceram. Int. 30 (2004) 2061.
[31] H.T. Zhu, C.Y. Zhang, Y.M. Tang, J.X. Wang, B. Ren, Y.S. Yin, Carbon 45 (2007) 226.
[32] C. Wang, W.L. Worrell, S. Park, J.M. Vohs, R.J. Gorte, J. Electrochem. Soc. 148 (2001) A864.
[33] J. Wang, Z. Lu, X. Huang, K. Chen, N. Ai, J. Hu, W. Su, J. Power Sources, in press.
[34] T.L. Reitz, H. Xiao, J. Power Sources 161 (2006) 437.
[35] P. Sarkar, P.S. Nicholson, J. Am. Ceram. Soc. 79 (1996) 1987.
[36] S.P. Jiang, J. Electrochem. Soc. 148 (2001) A887.
[37] S.P. Jiang, J.G. Love, L. Apateanu, Solid State Ionics 160 (2003) 15.
[38] F.T. Ciacchi, K.M. Crane, S.P.S. Badwal, Solid State Ionics 73 (1994) 49.
[39] J. Geyer, H. Kohlmuller,H. Landes, R. Stubner, in: U. Stimming, S.C. Singhal, H. Tagawa, W. Lehnert (Eds.), SOFC-V, vol. 97-40, Electrochem. Soc., Pennington, NJ, 1997, p. 585.
[40] S.P. Jiang, Y. Ramprakash, Solid State Ionics 122 (1999) 211.
[41] S.P. Jiang, J.G. Love, Y. Ramprakash, J. Power Sources 110 (2002) 201.
[42] E.P. Murray, T. Tsai, S.A. Barnett, Solid State Ionics 110 (1998) 235.
[43] M. Boaro, J.M. Vohs, R.J. Gorte, J. Am. Ceram. Soc. 86 (2003) 395.